Sol-air thermometer measurement of heat transfer coefficient at building outdoor surfaces

K. E. Anders Ohlsson[1]*, Ronny Östin[1],
and Thomas Olofsson[1]

[1]Umeå University, Department of Applied Physics and Electronics, S-90187 Umeå, Sweden
anders.ohlsson@umu.se, ronny.ostin@umu.se,
thomas.olofsson@umu.se

Abstract. There exists a building energy performance gap between theoretical simulations and the actual energy usage as measured. One potential reason for this gap might be a mismatch between predicted and measured values of the heat flux q through the building envelope. There is therefore a need to develop accurate and more cost-efficient methods for measurement of q.
The standard ISO 9869-1 states that, at the outdoor surface, $q = h_o(T_s - T_{env})$, where h_o is the overall heat transfer coefficient, including both convective and radiative components, T_{env} is the environmental temperature, and T_s is the temperature of the building surface. It has previously been shown that the sol-air thermometer (SAT) could be used for convenient measurement of T_{env} under dark conditions. In the present work, two SAT units, one heated and the other unheated, were employed for accurate outdoor measurements of h_o in cold winter climate. Validation was performed by comparison of results from the new method against measurements, where previously established methodology was used. With current operating conditions, the measurement uncertainty was estimated to be 3.0 % and 4.4 %, for h_o equal to 13 and 29 $Wm^{-2}K^{-1}$, respectively.
The new SAT steady-state method is more cost-effective compared to previous methodology, in that the former involves fewer input quantities (surface emissivity and infrared radiation temperature are unnecessary) to be measured, while giving the same h_o results, without any sacrifice in accuracy.
SAT methodology thus enables measurement of both T_{env} and h_o, which characterizes the building thermal environment, and supports estimation of q.

Keywords: Heat transfer coefficient, sol-air thermometer, environmental temperature, building energy performance gap.

1 Introduction

It is widely recognized, that there is often a gap between predicted and measured energy performance of buildings [1, 2]. Several different causes has been suggested for this energy performance gap. One possible cause is the use of inaccurate or inadequate input data for model predictions. Data which describes the thermal environment of the build-

ing is often of importance both at the design stage, for modelling of heat transfer between the building and its surroundings, and at the operational stage, as input to the heating (or cooling) control system. For evaluation of the energy performance gap, it is necessary to acquire relevant and accurate on-site measurement data for comparison against predicted values. In the present work, we developed a new measurement method, which can be used for accurate characterization of the building outdoor thermal environment. We start by showing how the thermal environment of the building could be described by a linear thermal network model, and how its parameters could be estimated, using the sol-air thermometer (SAT).

The heat flux q (Wm^{-2}) between the outer surface of the building envelope and the surrounding outdoor thermal environment could be modelled as:

$$q = h_o(T_s - T_{sa}) \tag{1}$$

, where h_o is the heat transfer coefficient, T_s is the building surface temperature, and T_{sa} is the sol-air temperature [3]. The heat flux q consists of three components: convective and net infrared radiative heat transfer, and incoming absorbed solar irradiation. Fig. 1 illustrates how q could be expressed as in Eq. (1), by simplification of a linear thermal network model of the thermal environment, and applying the Thevenins´ theorem of the circuit theory [4]. In this model, T_{sa} is the equivalent temperature of the thermal environment of the building surface, and is expressed as:

$$T_{sa} = T_{env} + \frac{\alpha I_s}{h_o} \tag{2}$$

, where T_{env} is the environmental temperature, α is the solar absorptivity, and I_s is the solar irradiation (Wm^{-2}). T_{env} consists of the weighted sum of the air temperature T_a and the mean radiant temperature T_r (longwave infrared radiation). The weights include the convective heat transfer coefficient h_c and the radiative heat transfer coefficient h_r, respectively. With $h_o = h_c + h_r$, we obtain:

$$T_{env} = \frac{h_c T_a + h_r T_r}{h_o}. \tag{3}$$

Under dark conditions, $I_s = 0$, and $T_{sa} = T_{env}$.

The SAT was originally designed for measurement of T_{sa} [5, 6], and its performance for that purpose has been evaluated [7, 8]. The SAT simply consists of a metal plate, with its back and side surfaces thermally insulated, i.e. there is ideally no conductive heat loss through the insulation material. The SAT is inserted into the building envelope, with the building surface aligned to the SAT front surface. These two surfaces are thereby exposed to the same thermal environment. The temperature of the SAT plate, T_{SAT}, is measured, often by insertion of a temperature probe into the plate. By applying Eq. (1) to the SAT front surface, we obtain:

$$q = h_o(T_{SAT} - T_{sa}) = 0 \tag{4}$$

, where $q = 0$ due to the insulation layer. We now see that $T_{SAT} = T_{sa}$, i.e. the SAT measures the sol-air temperature.

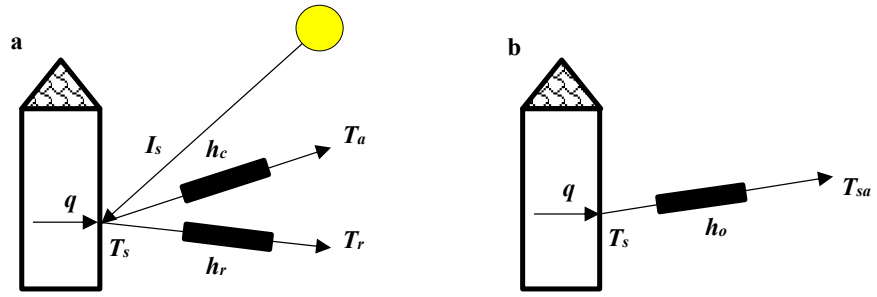

Fig. 1. Thermal network model for building surface and its environment. Thermal environment modelled (a) by solar irradiation, air temperature, and mean (infrared) radiant temperature, or (b) by the sol-air temperature, as driving forces for heat transfer.

At dark conditions, the SAT should enable direct measurement of T_{env}. The standard ISO 9869-1 claims that direct measurement of T_{env} cannot be performed (cf. section A.3.1 in [3]). However, we have recently used the SAT to directly measure T_{env} under dark and stable winter conditions [8].

SAT methodology could also be used for measurement of h_o at steady-state heat transfer. For this purpose, two SAT units (SAT1 and SAT0) were employed, and positioned side by side to expose them to the same thermal environment. These SAT units were heated electrically using resistive heater foils, and the supplied heater powers were p_1 and p_0 (Wm^{-2}), respectively. The energy balances for these units were:

$$p_1 = h_o(T_{SAT1} - T_{sa}) \tag{5}$$

$$p_0 = h_o(T_{SAT0} - T_{sa}). \tag{6}$$

Solving Eqs. (5) and (6) for h_o yields:

$$h_o = \frac{p_1 - p_0}{(T_{SAT1} - T_{SAT0})} \tag{7}$$

Eq. (7) is the basis for the new SAT method for measurement of h_o presented in this work (here named "SATss", the steady-state SAT method). The SATss method is a slight modification of the method used by Ito et al. [9] for measurement of the convective heat transfer coefficient h_c, given as:

$$h_c = \frac{p_1 - p_0 - \varepsilon_s \sigma (T_{SAT1}^4 - T_{SAT0}^4)}{(T_{SAT1} - T_{SAT0})} \tag{8}$$

, where ε_s is the emissivity of the SAT surface, and σ is the Stefan-Boltzmann constant ($\sigma = 5.67 \times 10^{-8}$ Wm^{-2}K^{-4}). We notice that, with the SATss method for measurement of h_o (Eq. 7)), there is no need for an estimate of ε_s, as is necessary for measurement of h_c using Eq. (8). In the present work, we selected p_0 to be zero (for measurement of T_{sa}, or T_{env} under darkness), i.e. SAT0 was left unheated.

In the present work, the objective was to demonstrate the accurate measurement of h_o, using two SAT units, and the SATss method expressed by Eq. (7). For validation of the SATss method, we performed simultaneous measurement of h_o using previously established methodology (here named the "ItoHr" method). In the ItoHr method, h_o was obtained as the sum $h_o = h_c + h_r$, where h_c was measured using the Ito method (Eq. (8)) and h_r was estimated as follows [3]: The infrared radiative heat flux q_r at the SAT front surface is given as:

$$q_r = \varepsilon_s \sigma (T_{SAT}^4 - T_r^4) = h_r (T_{SAT} - T_r) \tag{9}$$

By linearization of the T^4 terms around the average temperature $T_m = (T_{SAT} + T_r)/2$, we obtain:

$$h_r = 4\varepsilon_s \sigma T_m^3 \tag{10}$$

The measurement of h_r, using Eq. (10), thus requires estimates of both ε_s and T_r. In the present work, T_{SAT0} was used in T_m of Eq. (10).

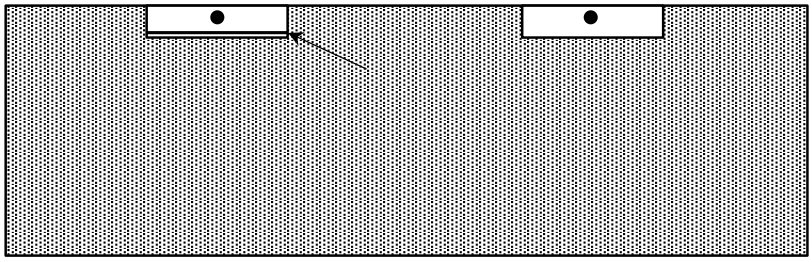

Fig. 2. Cross-sectional schematic view of the SAT pair, embedded in the insulation plate (grey). The arrow points to the heater foil (shown only for the heated SAT, but present in both). The black dots shows the positions for the SAT temperature sensors.

2 Experimental

A SAT unit, used in the present work, consisted of two circular copper plates, with 80 mm diameter, and with 12 mm and 1.5 mm thickness for the top and bottom plates respectively (see Fig. 2). A 0.3 mm thick resistive heater foil (polyimide Thermofoil™, Minco, Mineapolis, USA; 50.8×50.8 mm^2) was placed in between the plates, with thermal contact ensured by application of thermal paste (Wacker, paste P12). The heater resistance R_h was nominally 661 Ohm. The R_h, and its temperature dependence, was accurately determined in separate experiments.

The SAT unit was inserted into plates of extruded polystyrene insulation material (Sundolit XPS300BE, Sunde Group, Norway). The thermal conductivity of the insulation plate was ca 0.035 Wm^{-1}K^{-1}, and its thickness was 100 mm. Since the SAT front

surface was aligned with the surface of the insulation plate, there was a 86 mm thick insulation layer at the rear side of the SAT.

The front surface of the SAT was coated with a 0.1 mm thick layer of matt black paint (Nextel-Velvet coating 811-21; Mankiewicz Gebr., Hamburg, Germany). The emissivity of this Nextel coating has previously been determined to equal $\varepsilon_s = 0.943$ [10]. The temperature of the SAT was measured by insertion of a Pt-100 probe (4-wire, class A, 4 mm diameter, Jumo, Fulda, Germany) into a hole in the side of the top SAT plate.

The heat supplied (p_1) to the SAT1 unit was obtained by measuring the electrical DC voltage U supplied to its heater, and applying:

$$p_1 = \frac{U^2}{A_{SAT} R_h} \tag{11}$$

, where A_{SAT} (m^2) is the SAT front surface area. In Eq. (11), R_h was corrected to its value at the T_{SAT1} temperature. T_r was measured using a pyrgeometer (Hukseflux, model IR20-T1, Netherlands), while the absence of daytime levels of solar radiation was confirmed by measuring the solar irradiation I_s using a pyranometer (Hukseflux, model SR11) (see Fig. 3).

Fig. 3. Experimental setup. Three SAT units shown as black circle areas to the right in the figure, with SAT1 (heated) at the top and SAT0 (unheated) at the middle position). (The third SAT shown was not used in this work.) To the left side, the pyrgeometer (top) and the pyranometer (bottom) are seen.

All measurements (T_{SAT0}, T_{SAT1}, T_r, I_s, and U) were performed simultaneously using a data acquisition system (CompactDAQ and Labview software; National Instruments, USA), at a 0.02 Hz sampling frequency. Further details of the measurement system is given in [8, 11].

The series of measurements were performed outdoors on a roof terrace at Umeå University campus, Sweden, during the period from December 2016 to January 2017 (the present measurement series is identical to the one used as basis for work in ref. [8]). The insulation plate, with the two SAT units separated by a distance of ca 300 mm, was mounted side by side with the pyranometer and the pyrgeometer. These four measurement devices were all exposed to the same thermal environment (see Fig. 3).

The measured quantities (T_{SAT0}, T_{SAT1}, T_r, and U) were all estimated as the average value over a sampling period of time Δt, where environmental steady-state conditions prevailed. The criteria for selection of Δt also included a constant wind speed (measured at an on-site weather station, assuming that wind speed is constant also at the SAT surfaces), and the absence of daylight and precipitation (snow or rain). We also required that the Δt to always be larger than the time constant τ of the SAT, to allow time for its approach to a steady-state heat balance with its surroundings.

To ensure fulfillment of this requirement, we estimated τ, using a thermal network model. In this model, the SAT thermal capacitance C was estimated as:

$$C = \rho c_p V = \rho c_p L A_{SAT} \tag{12}$$

, where ρ is the SAT plate density (kg m^{-3}), c_p is its specific heat capacity (J kg^{-1}K^{-1}), L its thickness, and V its volume. The network model of SAT, and its thermal environment, then consists of the capacitor C in series with the resistance $R = 1/(A_{SAT} h_o)$, and with the time constant given by:

$$\tau = RC \tag{13}$$

In the present work, the SAT plate was made of copper, with $\rho = 8.93 \cdot 10^3$ kg m^{-3} and $c_p = 385$ J kg^{-1}K^{-1} (material property data obtained from [12]), and had $V = 6.78 \cdot 10^{-5}$ m^3. Finally, C was estimated to the value equal to 233 J K^{-1}.

3 Results and Discussion

Several series of measurements were performed outdoors under various winter weather conditions, and under darkness (cf. [8], where also wind speeds and weather observations are given). From these series, run sequences were extracted from time periods where measured temperature and radiation levels were constant, and where there was no precipitation (rain or snow). Table 1 lists the average temperature values obtained from each of 13 such runs, along with the heat supplied in each instance. Based on these data only, h_o was predicted by the SATss method (Eq. (7)), where two SAT units were used.

For purpose of method validation, h_o results from using the SATss method were compared against results obtained by using the ItoHr method (see section 1). In addition

to the measurement results shown in Table 1, the ItoHr method requires measured values for T_r, and an estimate of ε_s (see Table 2).

The method comparison is shown in Fig. 4. An ordinary linear regression yielded the equation $h_{o,ss} = 1.000 \cdot h_{o,itohr} + 0.43$, with standard errors equal to the values 0.008 and 0.16, for slope and intercept, respectively. The conclusion is here that h_o can be accurately measured, using the SATss method, except for a small constant bias, which is barely significant at the 95 % confidence level.

Table 1. Prediction of h_o, using the SAT steady-state (SATss) method (Eq. (7)), with $p_0 = 0$.

Run	T_{SAT0} (K)	T_{SAT1} (K)	p_1 (Wm^{-2})	$h_{o,ss}$ (Wm^{-2}K^{-1})
1	254.49	262.99	123.85	14.57
2	269.42	284.30	245.11	16.47
3	272.28	281.85	245.19	25.63
4	275.21	286.66	245.03	21.39
5	273.91	282.69	245.17	27.95
6	269.28	282.19	245.19	19.00
7	267.54	279.64	245.29	20.27
8	268.23	278.51	245.31	23.87
9	272.78	283.83	245.16	22.18
10	272.84	282.08	245.22	26.54
11	273.19	282.69	245.20	25.83
12	273.60	282.69	245.12	21.28
13	256.71	274.39	245.54	13.89

Table 2. Prediction of h_o, using the ItoHr method, where $h_o = h_c + h_r$, and data consisting of measured values of T_r, in addition to measured values given in Table 1. $\varepsilon_s = 0.943$.

Run	T_r (K)	h_c (Wm^{-2}K^{-1})	h_r (Wm^{-2}K^{-1})	$h_{o,itohr}$ (Wm^{-2}K^{-1})
1	244.82	10.86	3.33	14.19
2	264.99	11.93	4.08	16.01
3	261.14	21.08	4.06	25.14
4	274.74	16.65	4.45	21.10
5	272.40	23.34	4.36	27.70
6	257.57	14.52	3.91	18.43
7	255.49	15.89	3.83	19.71
8	255.10	19.50	3.83	23.33
9	269.08	17.57	4.25	21.83
10	259.86	21.97	4.04	26.01
11	259.69	21.24	4.05	25.29
12	273.06	16.61	4.37	20.98
13	255.74	9.88	3.60	13.48

The advantages with the SATss method for measurement of h_o in comparison to the established ItoHr method are that, in the former, T_r and ε_s need not to be known. Since the estimation of these two quantities requires use of extra resources, there is cost reduction associated with changing to the SATss method. Note also that here, for both

the SATss and ItoHr methods, the power supplied to the heater was measured electrically, and not by using a heat flow meter, as has previously been performed with the Ito method [9]. This probably improve the accuracy of the estimate of the supplied power, for both methods.

We here expressed measurement uncertainty following the GUM standard [13]. The relative measurement uncertainty for h_o, as estimated from the Eqs. (7) and (11), was equal to 3.0 % and 4.4 % for the lower and upper values, respectively, as shown in Fig. 4. At the lower end, the measurement uncertainty was limited by the uncertainty in estimation of A_{SAT}, while, at the upper end, the uncertainty in the measurement of SAT temperature difference was the limiting factor.

The time constant τ was estimated to equal between 28 min and 56 min, for the range of h_o values spanned by the 13 runs. The sampling time period Δt was always ≥ τ, with an average value of 3.6·τ.

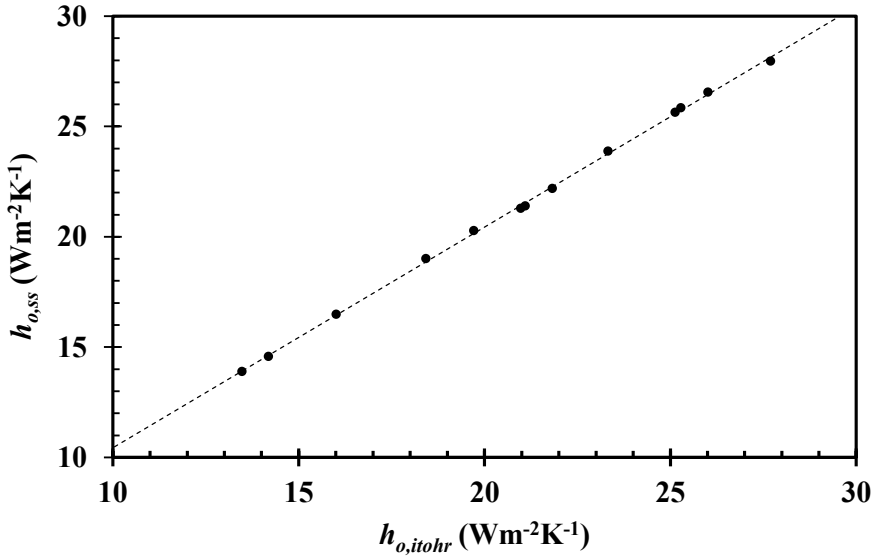

Fig. 4. Comparison of predicted values of h_o, obtained using the new SAT steady-state method ($h_{o,ss}$), against predictions obtained from using previously established methodology ($h_{o,itohr}$; the ItoHr method). An ordinary linear regression line is also given (dashed line).

4 Conclusions

We have designed a new and accurate method (named SATss) for measurement of h_o, using two SAT units. The SATss method requires less number of input data, compared to what was necessary using previously established methodology (ItoHr method), and could therefore be considered as more cost-efficient. Although the SATss method is simpler in its design, there is no sacrifice in accuracy.

SAT methodology now enables accurate measurement of both T_{env} and h_o. These two quantities together give an improved characterization of the building thermal environment, in terms of the simple network model, with the driving temperature (T_{env}) connected to the building surface by one single resistance ($R = 1/(A_{SAT}h_o)$). By providing accurate on-site measurement data, the SAT methodology has potential to reduce the building energy performance gap.

Acknowledgements. We gratefully acknowledge the financial support for this project from the Swedish Energy Agency, through IQ Samhällsbyggnad and the E2B2 program (project no. 39699-1), and the Kempe Foundations. We are also indebted to Fredrik Holmgren and Johan Haake for technical support in the construction of the experimental equipment.

References

1. Menezes AC, Cripps A, Bouchlaghem D, Buswell R: Predicted vs. actual energy performance of non-domestic buildings: Using post-occupancy evaluation data to reduce the performance gap. Applied Energy 97, 355-364 (2012).
2. De Wilde P: The gap between predicted and measured energy performance of buildings: A framework for investigation Automation in Construction 41, 40-49 (2014).
3. ISO 9869-1. Thermal insulation - Building elements - *In-situ* measurement of thermal resistance and thermal transmittance; Part 1: Heat flow meter method. 1 edn. ISO, Switzerland (2014).
4. Davies MG: The use of flux temperatures in thermal design. Building Services Engineering Research & Technology 2, 160-164 (1981).
5. Mackey CO, Wright LT: The sol-air thermometer - a new instrument. Transactions American Society of Heating and Ventilation Engineering 52, 271-282 (1946).
6. Muncey RW, Holden TS: The calculation of internal temperatures - A demonstration experiment. Building Science 2, 191-196 (1967).
7. Rao KR, Ballantyne ER: Some investigations on the Sol-Air temperature concept. CSIRO, Division of Building Research Technical Paper No. 27, Australia (1970).
8. Olofsson T, Ohlsson KEA, Östin R: Measurement of the environmental temperature using the sol-air thermometer. Energy Procedia (accepted), (2017).
9. Ito N, Kimura K, Oka J: A field experiment study on the convective heat transfer coefficient on exterior surface of a building . ASHRAE Transactions 78, 184-191 (1972).
10. Lohrengel J, Todtenhaupt R: Wärmeleitfähigkeit, gesamtemissionsgrade und spektrale emissionsgrade der beschichtung Nextel-Velvet-Coating 811-21 (RAL 900 15 tiefschwarz matt). PTB-Mittelungen 106(4), 259-265 (1996).
11. Ohlsson KEA, Östin R, Grundberg S, Olofsson T: Dynamic model for measurement of convective heat transfer coefficient at external building surfaces. Journal of Building Engineering 7, 239-245 (2016).
12. Incropera FP, DeWitt DP: Fundamentals of heat and mass transfer. 5 edn. Wiley, (2002).

13. JCGM 100: Evaluation of measurement data - Guide to the expression of uncertainty in measurement (GUM 1995 with minor correction). BIPM, ISO, Geneva (2008).